Supporting information for

Thermo-responsive Gold/poly(vinyl alcohol)-*b*-poly(*N*-vinylcaprolactam) Core/corona Nanoparticles as Drug Delivery System

Ji Liu,[a,c] Christophe Detrembleur,*[a] Marie Hurtgen,[a] Antoine Debuigne,[a] Marie-Claire De Pauw-Gillet,[b] Stéphane Mornet,[c] Etienne Duguet*[c] and Christine Jérôme*[a]

[a] *Center for Education and Research on Macromolecules (CERM), University of Liège, B6 Sart-Tilman, B-4000 Liège, Belgium.* christophe.detrembleur@ulg.ac.be and c.jerome@ulg.ac.be

[b] *Laboratory of Mammalian Cell Culture (GIGA-R), University of Liège, B6, Sart-Tilman, B-4000 Liège, Belgium*

[c] *CNRS, Univ. Bordeaux, ICMCB, UPR 9048, F-33600 Pessac, France.* duguet@icmcb-bordeaux.cnrs.fr

Supplemental experimental part

Materials

N-vinylcaprolactam (NVCL, 98%), 2,2,6,6-tetramethypiperidine-1-oxy (TEMPO, 98%), tetrachloroauric acid trihydrate ($HAuCl_4 \cdot 3H_2O$, ≥ 99.9%), sodium borohydride ($NaBH_4$, ≥ 99%), sodium hydroxide (NaOH, 98.5%), sodium chloride (NaCl, 98.0%), 2,2'-azobisisobutyronitrile (AIBN, 99%), potassium phosphate monobasic (KH_2PO_4, 98%), sodium phosphate dibasic (Na_2HPO_4, 98.5%), potassium chloride (KCl, 99.0%), fluorescein isothiocyanate isomer I (FITC, 90%), (2*R**,3*S**)-5- {[(2*R**)-3-(*tert*-butylamino)-2-hydroxypropyl]oxy}-1,2,3,4-tetrahydro -naphthalene-2,3-diol (Nadolol®, AR) and 4',6'-diamidino-2-phenylindole (DAPI, 98%) were purchased from *Aldrich*. Bis(acetylacetonato) cobalt(II) ($Co(acac)_2$, > 98%) and vinyl acetate (VAc, > 99%) were purchased form *Acros*. 2,2'-azo*bis*(4-methoxy-2,4- dimethyl valeronitrile) (V-70, 96%) was purchased from *Wako*. 3-(4,5-dimethyl- thiazol-2-yl)-5-(3-carboxymethoxy -phenyl)-2-(4-sulfophenyl)-2H-tetrazolium (MTS) was purchased from *Promega* (Madison, USA). DMEM (low glucose, without sodium pyruvate), *L*-glutamine, PBS buffer solution (without Ca^{2+} and Mg^{2+}), fetal bovine serum (FBS) and trypsin were obtained from *Biowhittaker* (Walkersville, MD). PBS buffer solution (with Ca^{2+} and Mg^{2+}), penicillin G, and streptomycin were purchased from *GIBCO BRL* (Gaithersburg, MD).

Characterization and measurement

Dynamic light scattering (DLS) measurements were carried out with a Malvern Instrument Nano-ZS, which were equipped with a He-Ne laser (λ = 663 nm) and scattering angle of 90°. The correlation function was analyzed via the CONTIN method, and D_h was determined using the Stokes-Einstein equation. The averaged D_h was obtained from three different runs. Standard deviation was used to evaluate the size polydispersity (PDI).

Transmission electron microscopy (TEM) was used to measure the size and size distribution of the nanoparticles with a Philips CM-100 microscope. A drop of the gold@PVOH-*b*-PNVCL NPs aqueous suspension was placed onto a carbon-coated copper grid and left to dry in air. The samples were negatively stained with uranyl acetate (2 *wt*.%, 2 min) before observation. The size distribution was analyzed by sampling *ca*. 200 particles on the TEM images.

X-ray diffraction (XRD) patterns of the gold@PVOH-*b*-PNVCL NPs were recorded by a Philips PW1700 diffractometer with Cu/Kα radiation (λ = 1.5418 Å).

Thermogravimetry analysis (TGA) traces of the gold@PVOH-*b*-PNVCL NPs, gold@PNVCL NPs and corresponding PVOH-*b*-PNVCL and PNVCL polymers were recorded from 20 to 600 °C at a heating rate of 20 °C min^{-1} in air with a TA Q100 Instrument.

Turbidity measurement of the PVOH-*b*-PNVCL copolymer, PNVCL homopolymer aqueous solutions (0.05 *wt*.%), gold@PVOH-*b*-PNVCL NPs and gold@PNVCL NPs aqueous suspension (50 μg mL^{-1}) was all carried out with a UV/*vis* spectrometer at a heating speed of 1 °C min^{-1} from 25 to 50 °C. Transmittance (700 nm) at different temperatures was plotted against the temperature, and LCST were taken from the point where the transmittance started to decrease.

UV/vis spectra of gold@PVOH-*b*-PNVCL or gold@PNVCL NPs aqueous suspension (50 μg mL^{-1}) were recorded between 200 and 900 nm from 25 to 50 °C with a Hitachi U-3300 UV/*vis* spectrophotometer.

X-ray photoelectron spectroscopy (XPS) of PVOH-*b*-PNVCL and gold@PVOH-*b*-PNVCL NPs was recorded with a VG Scientific 220 i-XL ESCALAB spectrometer at 100 W (10 kV and 10 mA), which was equipped with a non-monochromatized MgKα source (*hv* = 1253.6 eV). A pressure of 10^{-7} Pa was maintained in the chamber during analysis. The analyzed area was *ca*. 150 μm in diameter. The full spectra (0-1150 eV) were obtained with constant pass energy of 150 eV and high resolution spectra at constant pass energy of 40 eV. Charge neutralization was required

for insulating samples.

Fourier transform infrared spectroscopy (FTIR) analysis of the gold@PVOH-*b*-PNVCL NPs PVOH-*b*-PNVCL copolymers and $HAuCl_4$/PVOH-*b*-PNVCL mixture was recorded with a Perkin Elmer FTIR instrument. Samples were mixed and grinded with potassium bromide (KBr), and then pressed for FTIR analysis.

Supplemental result part

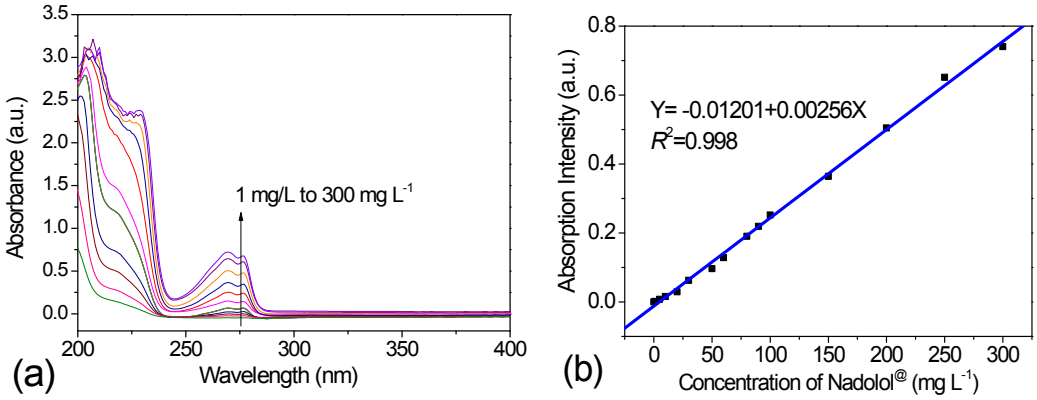

Figure S1. Calibration of Nadolol® concentrations via UV/*vis* spectrometry: UV/*vis* spectra of Nadolol® aqueous solution with different concentrations (a), and linear fitting of absorbance at 270 nm *vs*. concentration in the range of 1-300 mg L^{-1} (b).

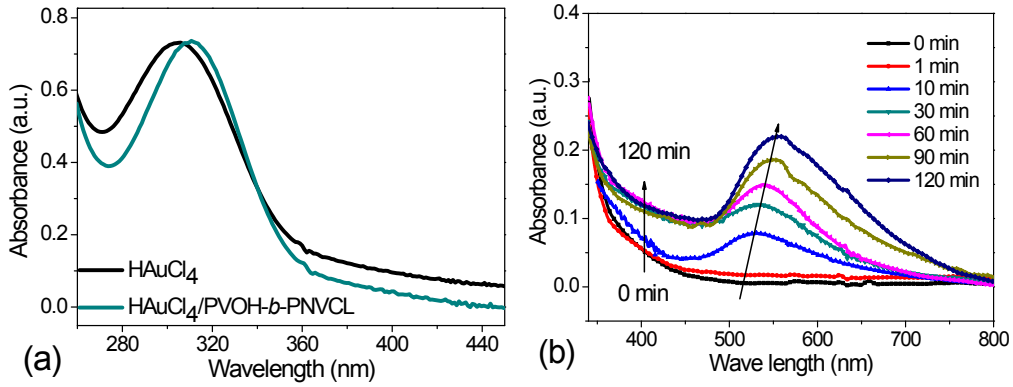

Figure S2. UV/*vis* spectra of $HAuCl_4$ and $HAuCl_4$/$PVOH_{226}$-*b*-$PNVCL_{494}$ mixture aqueous solutions (a), and representative *in-situ* UV/*vis* spectra of gold@$PVOH_{226}$-*b*-$PNVCL_{494}$ NPs (S#1) after addition of $NaBH_4$ at different reaction times (b).

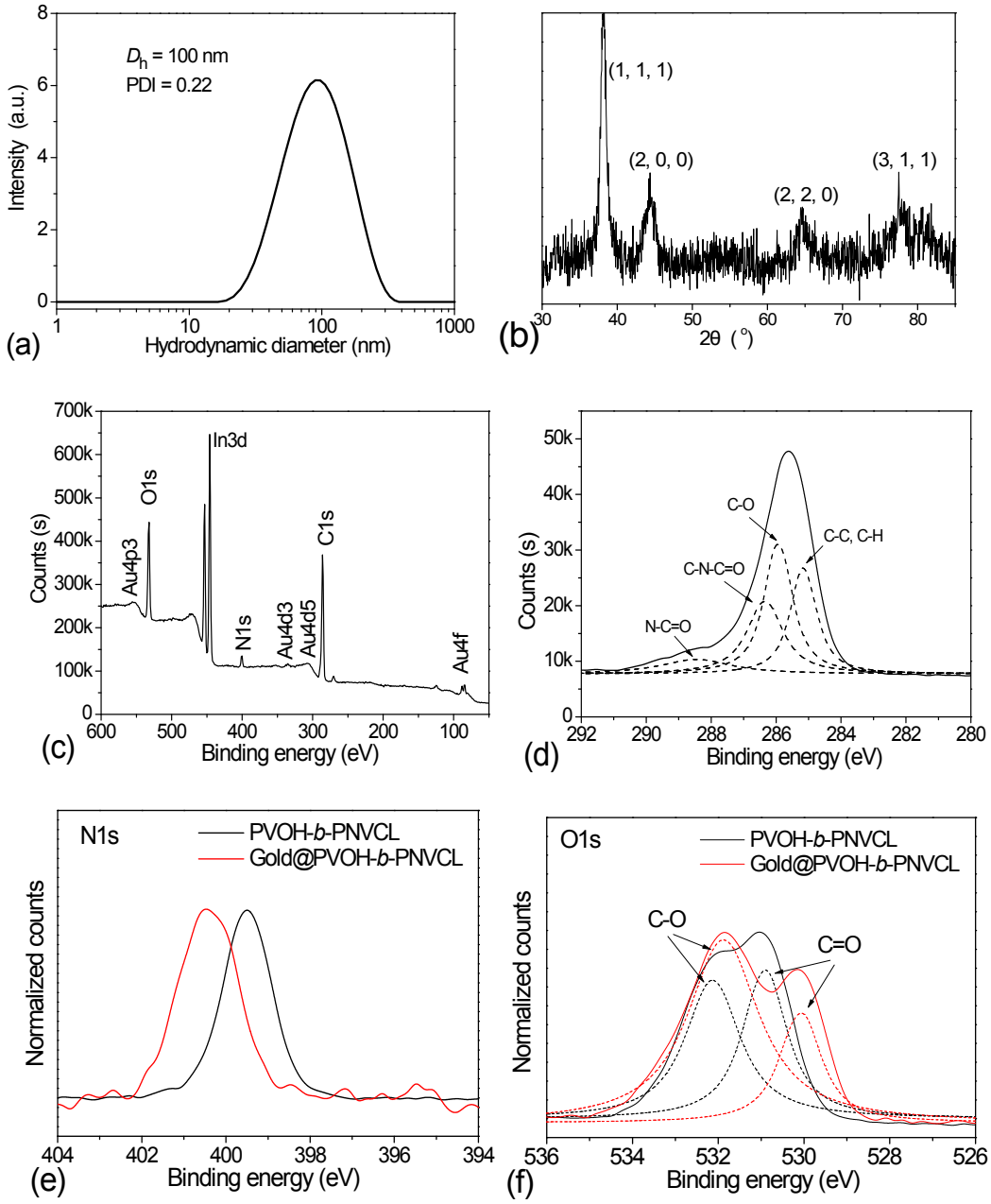

Figure S3. Intensity-averaged size distribution diagram of gold@PVOH-*b*-PNVCL NPs (S#1) aqueous suspension from DLS analysis (50 μg mL^{-1}, a) and XRD pattern (b) of gold@PVOH-*b*-PNVCL NPs (S#1); XPS spectra of gold@PVOH-*b*-PNVCL NPs (S#1): wide scan spectrum (c), peak-fitting of C1s signal of S#1 (d), comparison of N1s signal (e) and O1s signal (f) from pure PVOH-*b*-PNVCL (Polym#1, blank line) and gold@PVOH-*b*-PNVCL NPs (S#1, red line). The presence of gold cores was also confirmed by XRD, and the diffraction peaks were attributed to (111), (200), (220) and (311) crystal planes of the gold face centered cubic (fcc) lattices. In the wide scan XPS spectrum of the gold@PVOH-*b*-PNVCL NPs (c), the peaks arose at 84.1 and 87.9 eV were assigned to Au 4f7 and Au 4f5, respectively. In addition, Au 4d5, Au 4d3, and Au 4p3

peaks were also observed at 334.8, 353.3, and 545.6 eV, respectively. The XPS spectrum also showed intrinsic peaks of C 1s, O 1s and N 1s, which were attributed to the PVOH-*b*-PNVCL polymer coating (signals of In 3d originate from the subtract). The peak-fitting was performed on C 1s signal (d), and the peak at 285.0 eV was assigned to C-H and C-C chemical bonds, while peak at 286.0 eV for C-O, 286.3 eV for C-N-C=O and 288.4 eV for N-C=O bond, respectively. Peak-fitting was also performed on O1s signals (f), with peaks at 532.1 eV and 530.9 eV assigned to the C-O and C=O bonds from PVOH-*b*-PNVCL pure polymer, respectively; while 531.8 eV and 530.0 eV assigned to the C-O and C=O bonds from gold@PVOH-*b*-PNVCL pure polymer, respectively.

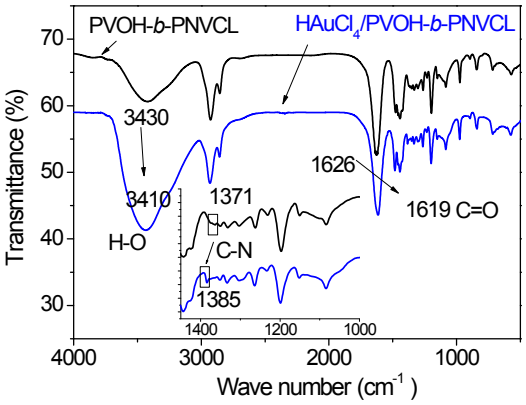

Figure S4. FTIR spectra of $HAuCl_4$/$PVOH_{226}$-*b*-$PNVCL_{494}$ mixture and pure $PVOH_{226}$-*b*-$PNVCL_{494}$ copolymer (inset: partially enlarged spectra from 1000 to 1450 cm^{-1}), as well as signal assignment of those transmission peaks of interest.

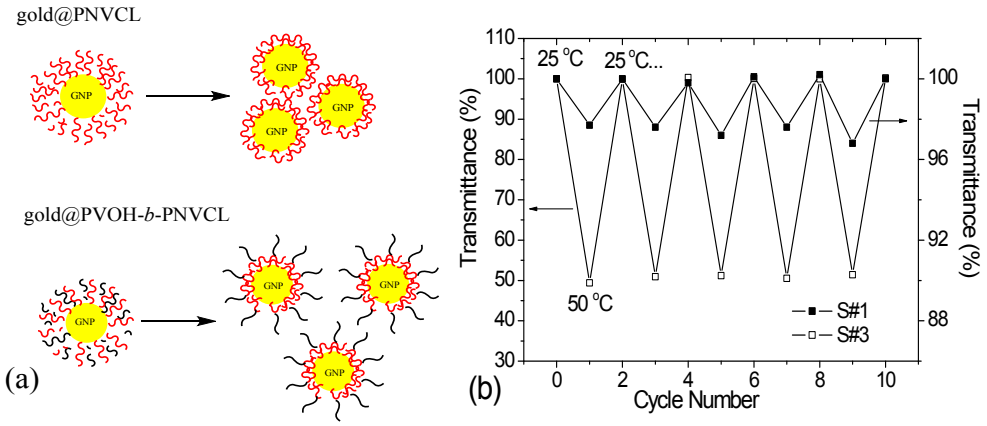

Figure S5. Schematic illustration of the conformation transition for gold@PNVCL and gold@PVOH-*b*-PNVCL NPs when temperature exceeds the LCST (a); evolution of transmittance

at 700 nm during the alternating cooing (25 °C)/heating (50 °C) treatment for gold@PVOH-*b*-PNVCL (S#1, solid) and gold@PNVCL (S#3, open) (b).

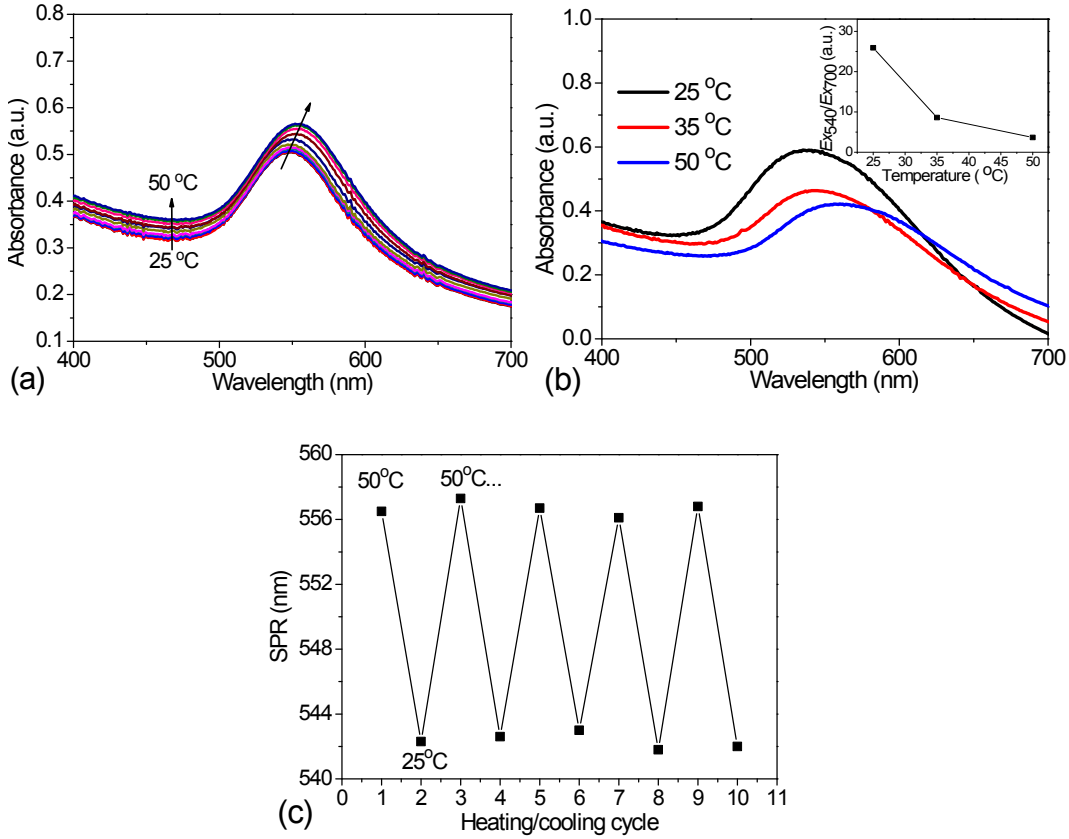

Figure S6. UV/*vis* spectra of gold@PVOH-*b*-PNVCL NPs (S#1) suspension between 25 and 50 °C (a) and gold@PNVCL (S#3) NPs suspension at 25, 35 and 50 °C (inset: the plotting of extinction ratio (Ex_{540}/Ex_{700}) as a function of temperature) (b); and evolution of SPR wave length under alternating heating (50 °C)/cooling (25 °C) treatment for gold@PVOH-*b*-PNVCL NPs (S#1, c). The solid line just serves as eye guidance.

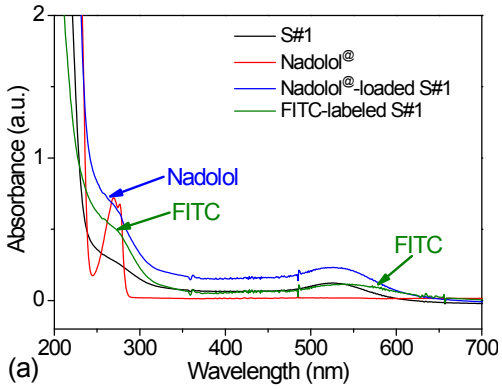

Figure S7. UV/*vis* spectra of the gold@PVOH-*b*-PNVCL NPs (S#1), pure Nadolol®, Nadolol®-loaded gold@PVOH-*b*-PNVCL NPs and FITC-labeled gold@PVOH-*b*-PNVCL NPs in aqueous medium

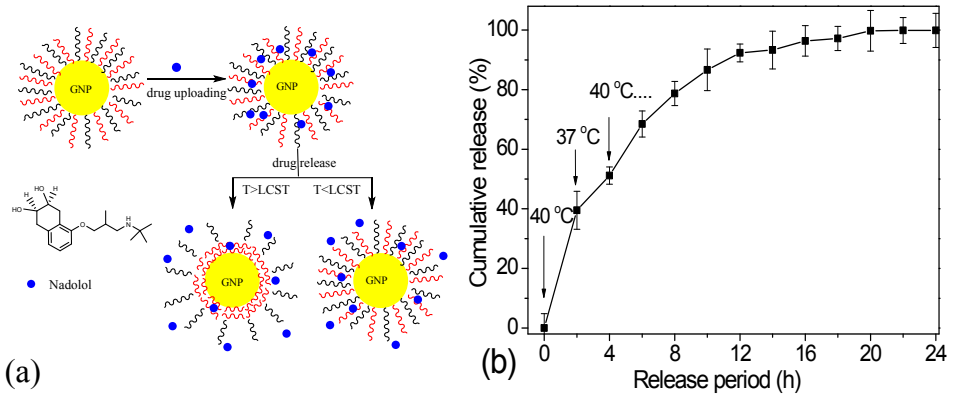

Figure S8. Scheme for the drug loading and thermo-induced release mechanism of Nadolol® from the gold@PVOH-*b*-PNVCL NPs below and above the LCST (a); and the cumulative release behavior of Nadolol® molecules from the Nadolol®-loaded gold@PVOH-*b*-PNVCL NPs (S#2) under alternating 40/37 °C heating/cooling treatment (b). The solid line just serves as eye guidance.

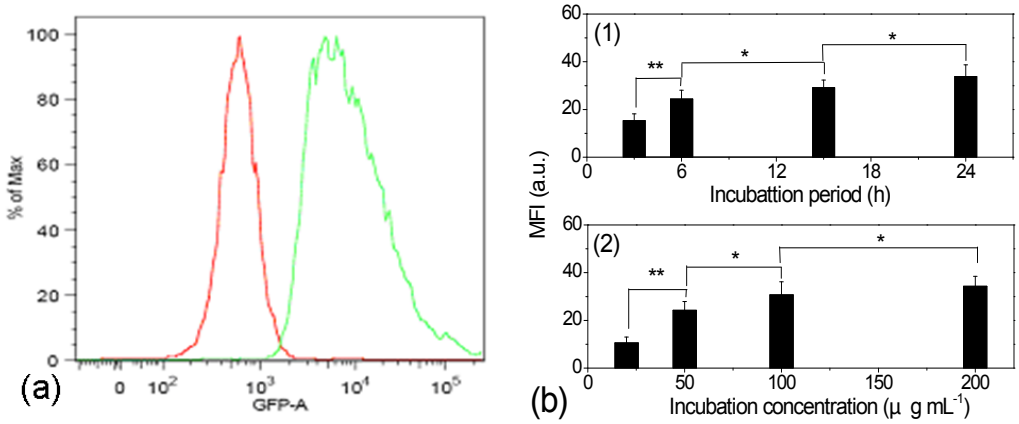

Figure S9. Cytofluorometric analysis of untreated MEL-5 cells (red, blank) and treated cells after incubation with FITC-labeled gold@PVOH-*b*-PNVCL NPs (S#1, 50 μg mL^{-1}, 6-h incubation, green); the number of cells (counts on *y*-axis) is plotted against the log of FITC absorption intensity (GFP-A on *x*-axis); and dependence of the mean fluorescence intensity (MFI) of treated MEL-5 cellson incubation period (S#1, incubation concentration of 50 μg mL^{-1}, b-1) and incubation concentration of FITC-labeled gold@PVOH-*b*-PNVCL NPs (S#1, 6-h incubation, b-2).